Real-time 3D UAV Path Planning in Dynamic Environments with Uncertainty

Zammit, Christian; Van Kampen, Erik Jan

DOI
10.1142/S2301385023500073

Publication date
2022

Document Version
Final published version

Published in
Unmanned Systems

Unmanned Systems, Vol. 0, No. 0 (2021) 1–18

Real-time 3D UAV Path Planning in Dynamic Environments with Uncertainty

Christian Zammit[a]*, Erik-Jan van Kampen[a] †

[a] *Delft University of Technology, The Netherlands*
E-mail: c.zammit@tudelft.nl

The integration of Unmanned Aerial Vehicles (UAVs) is being proposed in a spectrum of applications varying from military to civil. In these applications, UAVs are required to safely navigate in real-time in dynamic and uncertain environments. Uncertainty can be present in both the UAV itself and the environment. Through a literature study, this paper first identify, quantify and model different uncertainty sources using bounding shapes. Then, the UAV model, path planner parameters and four scenarios of different complexity are defined. To investigate the effect of uncertainty on path planning performance, uncertainty in obstacle position and orientation and UAV position is varied between 2% and 20% for each uncertainty source first separately and then concurrently. Results show a deterioration in path planning performance with the inclusion of both uncertainty types for all scenarios for both A* and the Rapidly-Exploring Random Tree (RRT) algorithms, especially for RRT. Faster and shorter paths with similar same success rates (>95%) result for the RRT algorithm with respect to the A* algorithm only for simple scenarios. The A* algorithm performs better than the RRT algorithm in complex scenarios.

Keywords: Path Planning; Real-time; Dynamic Environment; 3D; A*; RRT; Uncertainty.

1. Introduction

Unmanned Aerial Vehicles (UAVs) are becoming increasingly available for a wide spectrum of personal, industrial and military uses. In this regard, reliable, robust and autonomous guidance, navigation and control systems that can operate in real-time within obstacle-rich environments in the presence of uncertainties are required for UAVs to operate safely. The operating environment of a UAV may incorporate fixed and/or moving obstacles with different shape, size, orientation and speed. The obstacle characteristics are known, partially known or totally unknown to the UAV sensing system. In such time-varying scenarios, planning algorithms must ensure that the UAV reaches the predefined goal point using only onboard computational, sensory and fuel resources.

Planning can be segmented into two categories: Motion planning and Task planning.[1] Motion or path planning refers to the process of generating feasible and non-colliding paths from a predetermined start to a goal position. Task planning refers to a higher planning level which focuses on the task rather than vehicle dynamics and obstacle geometries.[1] In real environments with moving obstacles, planning algorithms need to construct and/or update path segments in real-time to reach the intermediate and final goal positions safely. In this regard, for the scope of this work path planning algorithms will be considered.

The environmental situation in dynamic environments is changing continuously and therefore the path planning system must re-assess already constructed path segments and if necessary re-evaluate path segments leading to intermediate and final goal positions to ensure obstacle avoidance and optimal navigation. Research stresses on the development of robust and generic path planning algorithms that can ensure obstacle avoidance in uncertain environments. In this regard, researchers remark that the problem of real-time path planning in uncertain environments is not fully studies.[2–4]

These motivations are key to the aim of this paper. The twofold aim of this paper is to assess the performance of the A* and the Rapidly-Exploring Random Tree (RRT) algorithms for real-time 3D UAV path planning in dynamic environments and consequently to investigate the effect of uncertainty in the same environment. A single UAV path planning system without knowledge of the obstacles' future path, will be considered in this paper. A dynamic environ-

*Visiting Researcher, Control & Simulation Department, Delft University of Technology, Kluyverweg 1, 2629 HS, Delft, The Netherlands
†Assistant Professor, Control & Simulation, Kluyverweg 1, 2629 HS, Delft, The Netherlands

ment with both fixed and moving obstacles will be considered, with moving obstacles having either a time-varying position, speed or orientation or any combination of these possibilities.

In real scenarios, uncertainty originating from different sources is only partially known or totally unknown to the path planner at the start of the planning process. Moreover, the real-time path planning algorithm must take account of time-variant uncertainty sources that can have a different effect as the UAV is navigating through the environment. In this regard, real-time path planning mandates that the path planning time is less than or equal to the time required by the UAV to traverse the same path.[5–7] The performance measures considered to assess the A* and RRT path planning algorithms in 3D real-time dynamic environments in the presence of uncertainty are: path length, planning time and success rate.

The work presented in this paper is founded on a previous paper presented in Unmanned Systems[8] that analysed the path planning response of graph-based and sampling-based algorithms for 3D path planning of UAVs. Based on the outcomes of this previous work, this paper will assess the path planning response of the A* and RRT algorithms in real-time 3D UAV path planning in dynamic environments in the presence of uncertainty. In this regard, the key contributions of this paper are:

(1) The design of a real-time A* and RRT path planning algorithm;
(2) The design of four translationally moving and rotating obstacles scenarios;
(3) The modelling of a set of uncertainties related to the UAV model and environment sensing, using bounding shapes;
(4) The analysis of the path planning responses of both the A* and RRT algorithms in all scenarios mentioned in 2 for a set of uncertainties mentioned in 3.

This paper will be organised as follows. Section 2 will present a review of the state-of-the-art in UAV path planning in dynamic environments including uncertainty. Section 3 will provide a summary of the A* and RRT algorithms, the path smoothing algorithm (applied only to the RRT algorithm) and a real-time path planning method, all presented in our previous work.[8–11]

Section 4 will define an obstacle generation algorithm, the environmental scenarios, the UAV model, the path planner parameter definitions and constraints and the uncertainty modelling and quantification rationale. Section 5 will present, discuss and analyse real-time 3D UAV path planning results for the UAV operating in dynamic environments in the presence of uncertainty. Section 6 will highlight the main outcomes, strengths and weaknesses of this work while recommending future endeavours.

2. Review on Path planning in dynamic environments in the presence of uncertainty

Autonomous path planning refers to the automatic process of constructing a collision free path to the goal position in the presence of both time invariant and time variant constraints, obstacles and threats (COT) and uncertainties.[8,9,12] This review will be divided into two sections: path planning in dynamic environments and path planning in the presence of uncertainty.

2.1. *Path planning in dynamic environments*

A wide range of time invariant and time variant COTs may pop-up when a UAV is moving through a dynamic environment.[13–15] These COTs include fuel, wind, altitude constraints, flight profile requirements, no fly zones and UAV kinematic and dynamic holonomic and non-holonomic constraints.[15–18]

Mac *et al.*[19] presented a path planning review spanning from 2000 to 2015 that concluded that only static obstacles and static targets are considered in 49% of the path planning projects. Both static and dynamic obstacles are included in only 18% of the path planning projects. Only 11% considered dynamic targets of which only 9% considered an adaptive UAV speed.[19] This shows although dynamic COTs are considered in a number of studies, the absolute majority considered a constant speed UAV.[19,20] The need for path planning in dynamic environments is highlighted in these reviews. This is attributed to the difficulty in path planning in dynamic environments.[19]

An autonomous path planner operating in a unknown and/or dynamic environment must re-plan in real-time or within a preset time window, using only onboard system information, a non-colliding path to the final goal point by also considering previously unknown COTs without assistance from an operator or a ground guidance system.[2,13–15,21–25] This *obvious* requirement,[14] is mandatory for an autonomous path planning system to be considered for real path planning applications.[26]

Normally, in path planning, the environmental space is assumed to be made up of two disjoint subsets, the free and the obstacle space subsets.[2] Different levels of environmental knowledge are provided to the path planning algorithms in different research studies. One category assumes that all environmental characteristics are known prior the start of the path planning process.[13,27] Another category assumes that the environment is totally unknown to the path planning algorithm.[24,28–30] A final category incorporates anything in between.[15,21,31]

Onboard computational power is limited in real-time UAV applications and the efficient use of it is essential for real UAV implementations.[21] In this regard, real-time COT modelling needed in time-variant environments for replanning requires efficient collision checks, efficient storage and fast inclusion and removal of environmental informa-

tion.[32] The computational burden of these requirements depends mainly on environmental complexity derived from obstacle occupancy. Obstacle modelling can be categorised into 4 main areas namely, Raw Data (vertices-edges sets), Kalman filtering, Bounding Volumes (Oriented Bounding Boxes) and Spatial Partitioning (Quadtrees).[21,33–35]

The problem of real-time path planning required for re-planning in dynamic environments was also addressed using classical methods including potential fields, cell decomposition, sub-goal networks and sampling-based algorithms.[19,36–38] Different performance measures including path length, computational time, clearance and deviation to the goal point are used to assess the validity of different path planning algorithms which are dependent on the mission requirements.[11,22,39]

2.2. *Path planning in the presence of uncertainty*

A path planning algorithm navigating a UAV in both indoor and outdoor environments, must mitigate with numerous factors with some incorporating uncertainty. These factors include environmental disturbances, partially known environments, limited on-board computational power, limited payload capacity and uncertainties in state and measurement.[3] A valid path planner must *always* ensure that the UAV safely navigates and stops in the goal region despite the presence of uncertainty in both sensing and control.[40] But, different researchers remark that uncertainty has not been fully studied.[2,41]

Robotic system uncertainties were categorised by LaValle *et. al*[76] in four categories: robot predictability uncertainty, robot sensing uncertainty, environmental sensing uncertainty and environmental predictability uncertainty. This study can be extended to 3D UAV scenarios. For the scope of this work, all uncertainty sources will be grouped into four main categories: UAV sensing system uncertainty,[2,40,54] UAV model uncertainty,[3,44,60] environmental sensing and prediction uncertainty[2,58,73] and communication uncertainty.[42]

The path planning algorithm's performance is highly dependent upon the fidelity of the uncertainty modelling methodology. Literature suggests that two main categories can be used to model uncertainty, namely Bounded Shapes and Probabilistic Distributions.[43,44] Bounded shapes technique use worst-case bounds are considered to set the limits of bounding shape.[44] These bounding volumes can have different shapes and can be modelled as time variant and time invariant. Oppositely, Probabilistic Distributions approximates parametric and agent states uncertainties using either a singular or a set of unbounded distribution functions.[44–46]

Uncertainties in certain parameters are sometimes interrelated with other environmental, mission and UAV modelling restrictions. Different studies define uncertainties prior mission initiation and add uncertainty weight at a predefined rate as the UAV is navigating towards the final goal position. Some studies focused on developing techniques to decrease this time propagated uncertainty with mission progression. A technique that address this difficulty uses previous data to reduce uncertainty in already explored volumes.[4] Another technique targets time propagated uncertainty attenuation by considering only the most recent sensory information.[47–49]

Different studies employed different path planning algorithms in the presence of uncertainty. The RRT algorithm and its variants were extensively used for path planning in the presence of uncertainty.[44,50–53] The A* algorithm is less used to plan paths in uncertain environments when compared to the RRT algorithm and its variants. This observation does not rule out the use of graph-based algorithms in uncertain environments. Other methods that were considered in path planning in uncertain environments include Partially Observable Markov Decision Process (POMDP),[54] Sliding Mode Control,[55,56] Linear and optimal Methods,[57] reactive path planning strategies,[3] Potential Fields and Probabilistic Maps,[58] Simultaneous Localisation and Mapping (SLAM)[2,59] Receding Horizon Control (RHC),[2] Q-learning,[60] Deep reinforcement Learning[61] and Shell Space Decomposition (SSD).[62]

3. The A*, RRT, Smoothing and Real-time Algorithms

This section will first present a brief description of the A* and RRT algorithms. These are the two most utilised graph-based and sampling-based methods. To mitigate with the RRT algorithm's non-optimality, a smoothing algorithm will be described. A summary of real-time path planning studies using the A* and RRT algorithms will conclude this section.

3.1. *The A* Algorithm*

Graph-based algorithms approximates the state space by an occupancy grid, setting points occupied by obstacles as unavailable grid points. If possible, Graph-based methods construct a path between start and goal positions using only available grid points.[63] A solution guarantee is only ensured if an adequate resolution is considered.[64]

The original A* algorithm determines the cost of neighbouring grid points using a heuristic evaluation function.[65] This function adds the cost from the current state to a projected future state to the cost from the latter to its respective goal point.[65,66] A detailed description of the A* algorithm is provided in our previous works.[8–11]

3.2. *The Rapidly-Exploring Random Tree (RRT) Algorithm*

Sampling-based methods construct a path from start to goal by connect non-occupied, randomly selected points in

the defined configuration space.[26,64] As opposed to graph-based techniques, sampling-based methods guarantee a solution in infinite time, if a solution exists.[64]

The original Rapidly-Exploring Random Tree (RRT) ultimately sets up a unidirectional tree from start to goal, by growing the tree and interconnecting tree branches. The tree branch construction process starts by randomly selecting an obstacle-free point. Then a point is defined at a predetermined distance from the nearest tree node, on the line connecting the nearest tree node with the randomly selected node. The tree branch will be the straight line connecting the defined point with the nearest tree node, only if, the tree branch does not collide with an obstacle. Tree branches are constructed until one branch reaches the goal point since the tree start at the start position.[67–69] Although the RRT algorithm is efficient in obstacle dense high-dimension situations it suffers in optimality and therefore it needs a post-planning smoothing algorithm.[69–71] Reference is made to our previous works for a more detailed review of the RRT algorithm and its variants.[8–11]

3.3. *The Smoothing Algorithm*

Both A* and RRT methods generate path points that when interconnected result in a non-colliding path from start to goal. Owing to the non optimality of the RRT algorithm, a post path planning smoothing algorithm is developed. For fair comparison, it was also applied to the A* algorithm.

The developed smoothing algorithm initiates by randomly selecting two path points from the set of path points defined by the path planning algorithm. Then two points on the straight line connecting the selected path points and their next path point are randomly selected. Provided that the straight line connecting these two points in non-colliding, the path points residing in between these two points are eliminated from the path. This will create shorter paths with lesser turns. This smoothing procedure is repeated, if the percentage reduction in path length is more than 1% in the last 20 iterates or less than 20 iterates were computed. Results from our previous work,[10] showed that for the A* algorithm a path length reduction between 1% to 10% results while a 25% to 45% reduction results for the RRT algorithm for only 1% of the path planning time. These results showed the validity of the relatively low complexity smoothing algorithm that can reduce path oscillations at a low computational expense. Refer to our previous work for a more detailed description and evaluation of this algorithm.[10,11]

3.4. *The Real-time Algorithm*

The requirement for real-time path planning is presented in literature in situations where the UAV is navigating in dynamic environments. This need is further emphasised in partially known or totally unknown environments in which the environmental situation is only fully known within the sensing range and the limited Field of View (FOV).[77–79] In our previous work a path planning algorithm emulating real-time response was developed.[11] The use of such algorithm is within the scope of this work and therefore the latter algorithm will be integrated within this study.

This real-time path planning algorithm first defines a non occupied intermediate goal point, a look-ahead distance from the current UAV position in the final goal point direction. The UAV's sensing range is directly proportional to the look-ahead distance. Then using either the A* or RRT algorithm, if possible, a path connecting the current UAV position with intermediate goal point is constructed. The UAV travelling distance along this intermediate path is governed by the maximum allocated intermediate time and UAV speed. The actuator systems' response is assumed to be unaffected by uncertainties and external disturbances and modelled with high fidelity. Moreover, the environment is assumed to remain static between intermediate path planning iterates since a short intermediate time is considered. A No Solution is set if either an intermediate non colliding path cannot be produced in the assigned time, the total time since the start of the mission exceeds the assigned time or the UAV collides with an obstacle. Section 4.3 provides a summary of the definitions of the different UAV parameters. A more in depth explanation of the real-time algorithm and its path planning performance characteristics for both A* and RRT algorithms is provided in our previous work.[11]

4. Environmental and Uncertainty Modelling

This section will initiate with the definition of the obstacle generation algorithm followed by the developed environmental scenarios. A description of the UAV model and the path planner parameter constraints will follow. This section will conclude with the percentage uncertainty bound definitions of both UAV position and obstacles.

4.1. *Obstacle generation algorithm*

Literature suggests that every real-life obstacle can be modelled using regular shapes.[12,14,23,39] This algorithm first retrieves the characteristics and position of each obstacle at initiation stage and at future time intervals. Real-time path planning requires the sensing and modelling systems to estimate the environment independently from the path planning algorithm. Therefore the environment is estimated prior the initiation of the real-time path planning tests.

Closed or open obstacle shapes are constructed by interconnecting a set of planes. Each obstacle shape is reproduced a number of predetermined times. Each replica is then randomly placed within the environmental space. A random rotation in all 3 different axis about a randomly-generated line is added for each copy, in case obstacle rotation is considered. To define the position and orientation of each obstacle at progressing time stamps, a random shift

by a random distance and direction and/or a random rotation for each obstacle copy is performed for a predetermined times. This results in obstacles experiencing a time-varying speed, roll, pitch and yaw. For every change in obstacle state it is assumed that a time window has passed. During this time window the UAV would move from its current point to a new point along the intermediate path. To ensure obstacle avoidance, it is required that the maximum distance that the UAV can move is longer than the maximum distance obstacles cam move. If obstacle future movement is known apriori, obstacles with faster movement can be evaded by the UAV.

4.2. *Environmental Scenarios*

The path planning performance of both the A* and RRT algorithms are assessed using four different complexity scenarios. In the obstacle environment implementation three shapes were considered, namely a cube, the V obstacle and 2D planes with small windows. The obstacle characteristics of which are tabulated in Table 1. The same occupancy chance is considered in all the environment when randomly placing cubes and V obstacles. Throughout the obstacle modelling and environment design process, modular unitless dimensions are used so as to ease scaling to real UAV path planning situations. The four environmental scenarios are constructed, as described in the following list.

- Scenario 1: Ten 0.1x0.1x0.1 cubes without rotation;
- Scenario 2: Ten 0.1x0.1x0.1 cubes with different random rotation at initiation stage and different time varying random rotation with time iterates increments;
- Scenario 3: Ten V obstacles each made up of two 0.1x0.112 planes, touching with each other with a common side, having a 53° the. A random rotation as described in Scenario 2 is considered. This plane size and configuration is considered since it exactly fits into a 0.1x0.1x0.1 cube; and
- Scenario 4: The combination of Scenarios 2 and 3 together with two X-Z planes, 0.4 distant from each other with a 0.2x0.2 square window.

These tests are designed starting with the simplest translationally moving and non-rotating cube case with each test scenario adding path planning difficulty. It is assumed that, all shapes except the 2D planes in Scenario 4 move at different time varying speeds in random directions.

Figure 1 shows an instance for each scenario at an arbitrary time stamp neglecting uncertainty constraints. The obstacle positions in each scenario will vary in subsequent iterates since the obstacles are experiencing translational and rotational movement.

4.3. *Path planning parameter definitions*

Table 2 tabulates the nominal path planning parameter values, derived from our previous work,[11] which was based on the evaluation of real UAV characteristics.

A cubic environmental space of 1x1x1 is constructed with a fixed start point at (0,-0.5,0) and fixed goal point at (0,0.5,0). These characteristics are considered in all tests. In all path planning tests using the A* algorithm, the environmental space and start and goal points are all randomly displaced between 0 and half the distance between grid positions. This process is intended to cancel the ripple in path length as analysed in.[10]

For graph-based algorithms, including the A*, the resolution is defined as the number of grid points per unit dimension. For sampling-based algorithms, including the RRT, all non-occupied points can be used for path planning. For an impartial comparison between the A* and RRT algorithms, the distance between grid positions for A* and the tree branch length for RRT are assigned the same value. The distance to travel per iterate (d_{s_step}) is set to two times the distance between grid positions for A* and the tree branch length for RRT. The the distance between the current UAV position and a possible intermediate goal point (d_{int_goal}) is then set to two times d_{s_step}. For the path planner to visualise the second obstacle plane window, in the mixed case, d_{int_goal} has to be increased to 0.6[-] from the initial 0.4[-]. The time required for the UAV to move d_{s_step} is defined as the maximum time to generate a path segment ($t_{iterate\_max}$). The maximum time to generate the whole path ($t_{path\_gen\_max}$) is set at 10 times $t_{iterate\_max}$. The distance reduction factor is included to decrease the respective distance in situations where the prospective intermediate goal points and/or the prospective future UAV position will not be set on an obstacle-free point. UAV speed is assumed constant during each test situation. In different tests, UAV speed is varied from 0.01[-/s] to 0.1[-/s] in 0.01[-/s] steps. The [-] sign imply that distances are modular. These real-time path planning algorithm parameters are set based on performance analysis in.[11]

4.4. *Bounded Uncertainty Definitions and Quantification*

The literature review presented in Section 2, categorised uncertainty based on four main uncertainty categories. These are uncertainty in sensing systems, uncertainty in UAV model, uncertainty in the environment and uncertainty in communication. The former three uncertainty categories will influence the obstacles and UAV's position and orientation within the UAV sensing volume. In this regard, these three uncertainty categories are integrated within UAV positional uncertainty and obstacle positional and orientation uncertainties as shown in Figure 2. Also, Figure 2 show that communication uncertainty is not considered in this study, since a standalone UAV is assumed. Moreover, orientation uncertainty is not considered since the UAV is approximated by a point model.

As explained in literature, both bounded shapes and probabilistic uncertainty modelling techniques are potential candidates for uncertainty modelling in both UAV and

Table 1. Obstacle characteristics

Shape	Size	Number of Planes	Open/Closed
Cube	0.1x0.1x0.1	6	Closed
V obstacle	0.112x0.1	2; (53^o between planes)	Open
Plane with window	1x1	1; (0.2x0.2 window)	Open

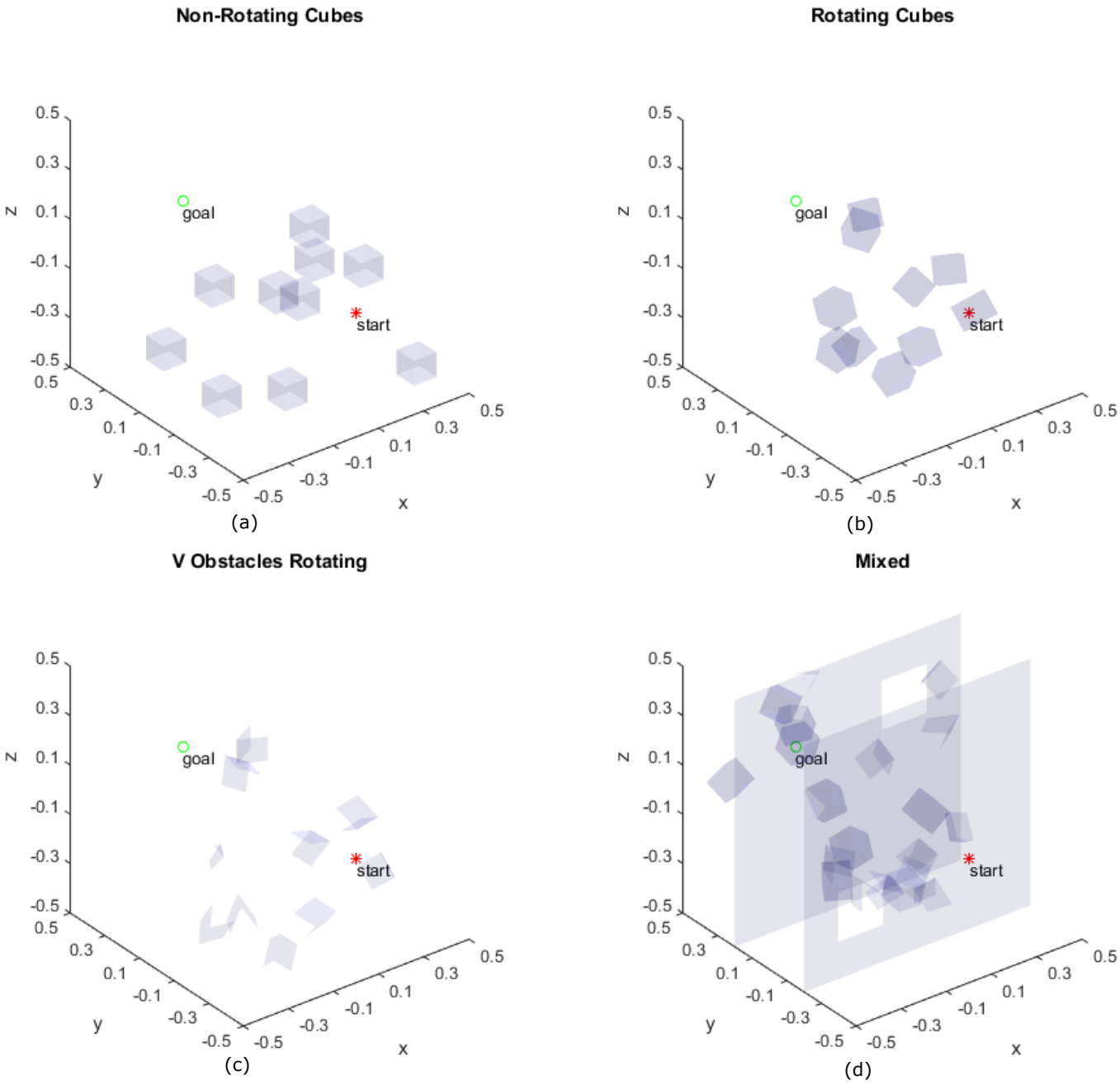

Fig. 1. Obstacle scenarios: (a) Non-rotating cubes, (b) Rotating cubes, (c) Rotating V obstacles and (d) Mixed case scenarios.

obstacle positions. All grid and selected points within the UAV sensing volume can have only two states namely, occupied or non-occupied when the bounded shape technique is considered. Oppositely, probabilistic techniques

Table 2. Real-time path planning algorithm parameter assignment

Parameter	Nominal Value	Units
Resolution (res) for A*	21	[-]
Step size for RRT (d_{step_RRT})	$\frac{1}{21-1} = 0.05$	[-]
Distance to travel per iterate (d_{s_step})	$\frac{2}{res-1} = 0.1$	[-]
Distance between current UAV position and prospective new intermediate goal point (d_{int_goal})	0.4 and 0.6 for Mixed case scenario	[-]
Maximum time to generate path segment ($t_{iterate\_max}$)	$\frac{d_{s\_step} \times 60 \times 60}{10 \times v_{UAV}}$	s
Maximum time to generate path ($t_{path\_gen\_max}$)	$10 \times t_{iterate\_max}$	s
Distance reduction factor (d_{factor})	0.8	[-]

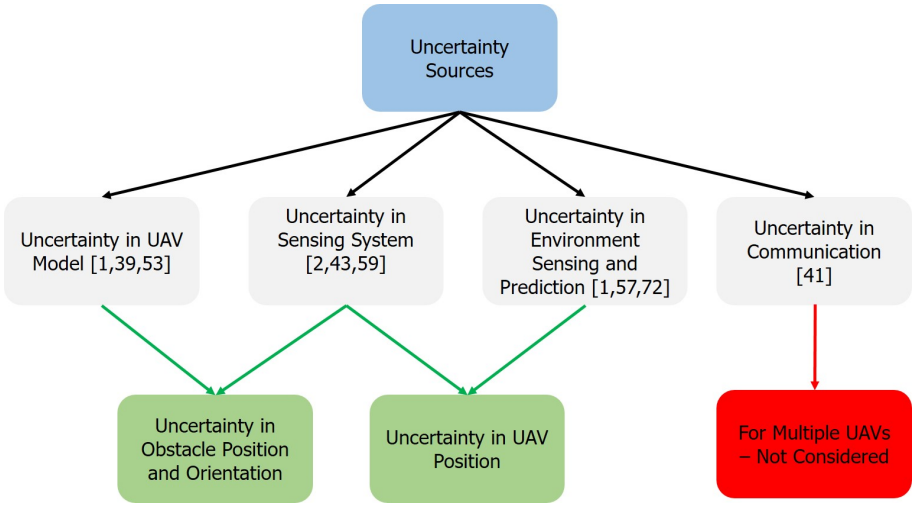

Fig. 2. Illustration of uncertainty sources categorisation, showing how these uncertainty sources are integrated within the developed uncertainty modelling environment

consider a probability based distribution function for every point. A threshold will then determine whether each point is occupied or non-occupied. This threshold must be defined in real-time or prior mission initiation. Probabilistic methods will result in higher computational requirements as opposed to bounded shape techniques. For this study, bounded shape techniques will construct a bounded shape enclosing obstacles or the UAV position with an added uncertainty factor and presumes that the environmental space within bounds is occupied with certainty.

Figure 3 shows enclosures bounding a set of obstacles and a spherical bound surrounding the UAV position. The constructed 3D enclosures add an equidistant limit from the true obstacle edges. A sphere enclosing the UAV position is considered for impartial analysis since it creates an equal uncertainty bound in all 3 dimensions. For the scope of this study, uncertainty in UAV's position and obstacle position and orientation are assumed invariant. This assumption is valid since the precision and accuracy of the UAV sensing and positional systems remain constant within the look-ahead distance volume.

During real-time path planning, it is assumed that the true UAV position can be located, with the same probability, at any point within the spherical bound. This spherical time invariant bound includes the worst case UAV positional deviation. In this regard, the current UAV position in the next iteration is randomly chosen from within the bound enclosing the future UAV position, with the latter defined on the path constructed in the last iteration. The UAV position and obstacle movement and rotation definition process is computed for every UAV step movement. Each test case scenario is repeated for 100 times for every UAV speed considered.

A percentage of the obstacle volume is considered in the quantification of uncertainty bounds for 3D obstacles, namely cubes. For V obstacles, constructed from two 2D planes, 10 planes are used to define the associated uncertainty bounds so as to totally enclose the V obstacle as shown in Figure 3 (b). Figure 3 (b).(i) shows the V obstacle's 3D profile while (b).(ii) and (b).(iii) shows the same V obstacle with uncertainty bounds from the X-Y and X-Z perspective, respectively. The mixed scenario incorporates cubes, V obstacles and 2D planes with windows. The uncertainty bounds of cubes and V obstacles are defined as described earlier. For the 2D planes with windows, uncertainty bounds are defined by two identical planes but with

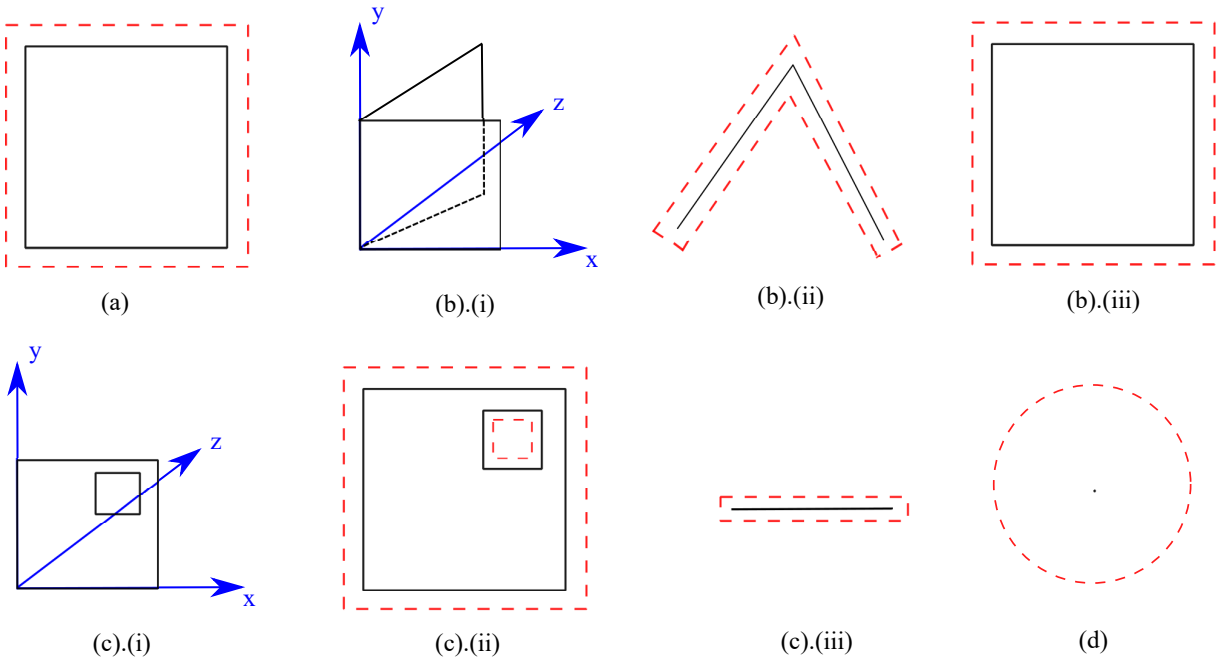

Fig. 3. Illustrations of uncertainty bounds for: (a) Cube, (b) V obstacle, (c) X-Z planes with window openings and (d) UAV position.

smaller windows displaced equidistantly to opposite sides from original 2D plane. The 2D plane is enclosed to create a 3D uncertainty bound, by connecting the edges of the two identical planes as shown in Figure 3 (c). In this regard, Figure 3 (c).(i) illustrates a 3D profile of the X-Z window plane while (c).(ii) and (c).(iii) illustrate the uncertainty bounds from the X-Z and X-Y perspective, respectively. The nominal uncertainty percentage values of obstacle shapes are decided based on literature.[72,73] Figure 3 (d) shows the spherical bound defining the maximum UAV positional uncertainty. The spherical bound radius is calculated by the multiplication of the distance moved by the UAV in one iterate d_{s_step} and the literature-derived uncertainty.[60,72]

In all tests, percentage uncertainty in obstacle position and/or UAV position ranges from 2% to 20% and is increased in 2% steps when uncertainty effects on path planning performance is being assessed. In all other cases uncertainty is set to 0%.

5. Results

The 3D real-time A* and RRT path planning algorithms, the obstacle environments and the UAV positional and obstacles' positional and orientation uncertainties explained earlier are all implemented in MATLAB. Testing is done using a 3.2GHz Intel Xeon ES-1650 processor. The performance measures for path planning analysis are the path length, computational time and success rates. When the effects of uncertainty are evaluated the UAV speed is set at 0.05[-/s]. In all other cases, UAV speed ranges from 0.01[-/s] to 0.1[-/s] in 0.01[-/s] steps. For all tests, the nominal path planning parameters values listed in Table 2 are considered.

In case, that an intermediate path could not be constructed since the path construction time exceeds the path traversal time (real-time path planning requirement), such test case is considered as unsuccessful and labelled: *"Int. Time Exc."*. Similarly, if the total time to construct and traverse the path exceeds the predetermined time defined in Table 2, such test case is considered as unsuccessful and labelled: *"Max. Time Exc."*. All other unsuccessful cases are labelled: *"No Path"*.

5.1. *A* and RRT without uncertainty*

This section assesses the real-time path planning performance of the A* and RRT algorithms in translationally moving and rotating obstacle environments without uncertainty. Figure 4 shows the path length, computational time and success rate results for both A* and RRT algorithms as UAV speed increases from 0.01[-/s] to 0.1[-/s] keeping the path planning parameters listed in Table 2 constant.

Two contrasting rationales were considered in our previous work[74] in case an obstacle-free path to an intermediate goal point is impossible or when the prospective new UAV position resides on an obstacle. Two solutions were proposed in this situation. In the first solution the real-time planner re-assign the new UAV current position to its previous state until an obstacle-free path to an intermediate goal point is possible. The real-time planner also waits in situations where the new prospective UAV position is available

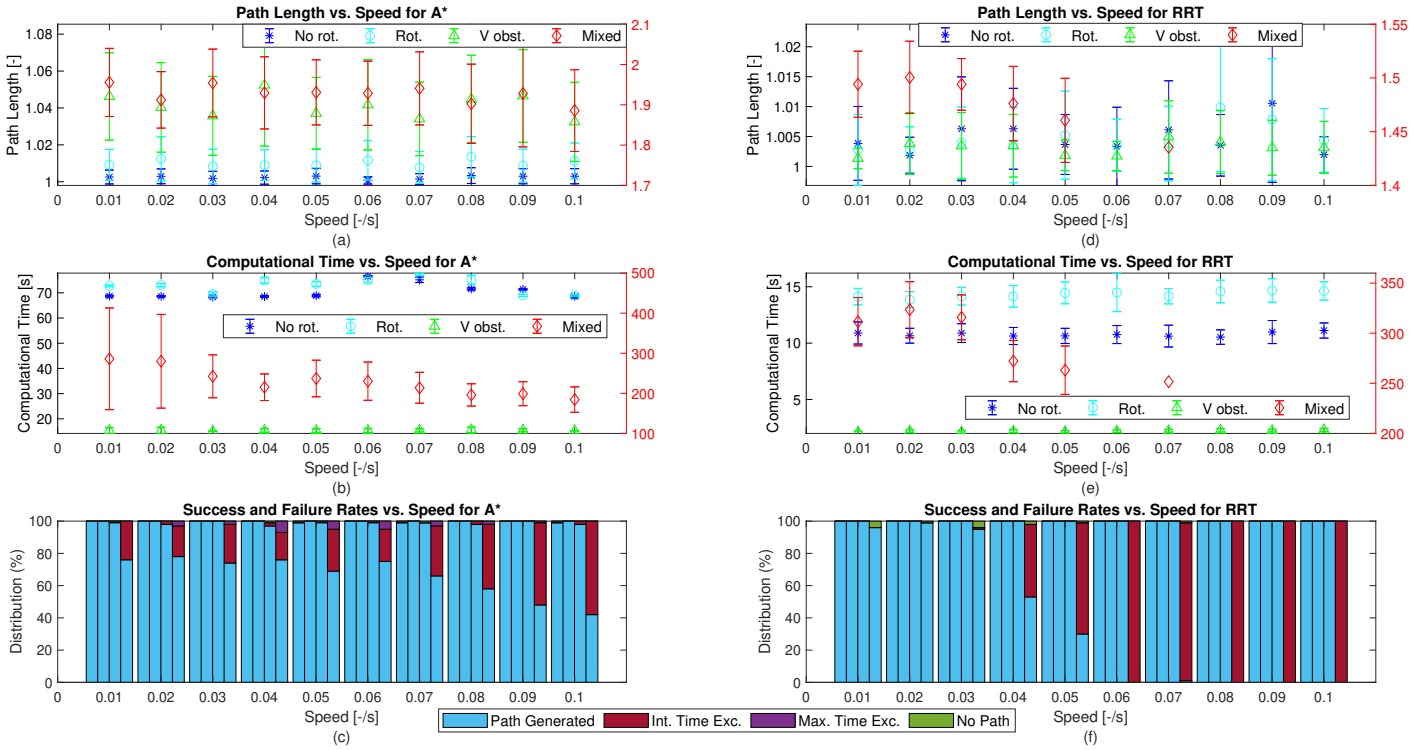

Fig. 4. Performance parameters vs. speed: (a) Path Length, (b) Computational Time, (c) Success rates for A* and (d) Path Length, (e) Computational Time and (f) Success rates for RRT for 100 iterates with 95% confidence interval. The left side black vertical axis relates to the non-rotating cube, rotating cube and rotating V-obstacle case while the right side, red vertical axis relates to the Mixed case. The set of four columns in (c) and (f) represent the non-rotating cube, rotating cube, rotating V-obstacle and the Mixed case scenarios. Adapted from[74]

but a path cannot be constructed due to obstacles (waiting variant). In the second solution, the real-time planner does not wait, but instead defines a new intermediate goal point or a new UAV position (controlled by d_{factor}) nearer to the current UAV position (moving variant). An analysis concluded that the moving variant solution resulted in better overall performance in terms of all performance measures than the waiting variant solution. Therefore moving variant is considered for this analysis.

From an analysis of Figure 4 it can be concluded that all scenarios, except for the mixed case, produce a path very close to 1 (straight line distance from start to goal) for both algorithms for whole range of speeds considered. The cube without rotation resulted in the shortest path length followed by the rotating cube and V obstacle scenarios, respectively for both algorithms and the range of UAV speeds. A significant path length increase results in the Mixed case using both A* and RRT algorithms for all speeds. This results since the planner is required to pass through two opposite-sided windows on two different planes as shown in Figure 1 (d). The overall path length for A* is longer than RRT for all scenarios and speeds under analysis. Moreover, speed only limits the maximum intermediate and total time entitlement and is independent of path length.

The difference in both path length and computational time between Scenarios 1 and 2 is small, but not negligible, compared with the Mixed case scenario. In fact, the path length is 0.8% and 0% longer and computational time is 3.3% and 33% longer for the rotating cube case with respect to the non-rotating cube case, for A* and RRT respectively. Both Scenarios 1 and 2 need to be considered to directly assess the effect of rotation on path planning performance.

For scenarios 1 to 3, the path planning time of the A* algorithm is longer by 5 to 7 times with reference to the RRT algorithm. For the mixed scenario, the path planning time for A* is 18% shorter with respect to RRT for UAV speeds from 0.01[-]/s to 0.05[-]/s. This results since the RRT success rate is close to 0% at higher UAV speeds. It can be concluded that path planning time is independent of UAV speed for both path planning algorithms. The path planning time for both path planning algorithms is lowest in the V obstacle case, followed by the non-rotating

and rotating cube cases and the mixed case experiencing a large increase. This outcome shows the direct relationship between scenario complexity and computational requirements. In fact, the V obstacle consists of only two 2D planes while 6 planes are used to construct cubes with an internally occupied space. This larger computational demand for A* with respect to RRT is a consequence of the A*'s graph-based rationale and its ripple reduction algorithm that requires re-modelling in every iteration.

In terms of path length variance, A* is 28% smaller and 89%, 4 and 2 times larger than RRT for scenarios 1 to 4 respectively. A similar analysis for computational time show that A* is 44% and 45% smaller and 5 and 3 times larger than RRT in terms of variance for scenarios 1 to 4 respectively.

Both path planning algorithms result in an almost 100% success rate for scenarios 1 to 3. A 100% success rate results for RRT and a minimum 95% success rate results for A*. In the mixed case, a minimum of 95% success rate is recorded for RRT for UAV speeds up to 0.03[-/s], reducing to 0% with increase in UAV speed. The A* success rate is lower than RRT's at low speeds but retained a minimum success rate of 40% at the highest UAV speed as opposed to the success rate of RRT that dropped to 0%. For a deeper analysis refer to.[74]

In terms of success rate both algorithms exhibit a near 100% success rate for the first three scenarios with RRT exhibiting a 100% success rate, while A* achieved a minimum of 95% success rate. For the Mixed case, the RRT achieved a success rate of a minimum of 95% for speeds from 0.01[-/s] to 0.03[-/s], deteriorating to 0% as speed increases. The A* algorithm, never achieved this high success rate of the RRT algorithm, but maintained a success rate above 40% at the highest speed as opposed to the success rate of RRT that dropped to 0%. For further analysis of these results refer to.[74]

The path planning performance analysis show that both A* and RRT algorithms can operate in real-time path planning environments with translationally moving and rotating obstacles provided that an adequate intermediate and total time is allocated.

The inclusion of UAV positional uncertainty as described in Section 4 will follow.

5.2. *A* and RRT with uncertainty in UAV position*

The UAV positional uncertainty is a percentage of the predetermined UAV movement per iterate. This is randomly added during the calculation of the true UAV position for the next iterate. The path planning performance of both A* and RRT algorithms with different UAV positional uncertainties is illustrated in Figure 5. During these tests, two inter-linked parameters are concurrently changing. The first parameter is the maximum UAV positional uncertainty that determines the minimum UAV distance to obstacles for non-collision. The second parameter is the random movement between 0[-] and the maximum UAV positional uncertainty (first parameter) added in the calculation of the UAV position for the next iterate.

For the A* algorithm, the cube with no rotation case results in the shortest path length, followed by the rotating cube, V obstacle and mixed cases, respectively. For the RRT algorithm, the V obstacle scenario generates the shortest path length, followed by the non-rotating cube, rotating cube and mixed cases, respectively. The path length in scenarios 1 to 3 is small. This ranking is in line with the no uncertainty test cases for the A* algorithm but differs for RRT due to the V obstacle's large path performance deterioration. Path length for the mixed scenario is 1.5 to 2 times longer with respect to Scenarios 1 to 3 for both path planning algorithms. It can be concluded from Figure 5 (a) and (d) that path length increases with increase in percentage UAV positional uncertainty for both algorithms and all scenarios.

The V obstacle case resulted in the lowest computational time for the whole range of uncertainties for both path planning algorithms. This results since in the V obstacle case, only two planes per shape are checked for potential collisions while in the cube cases, six planes and the cube interior requires collision checks. The A* algorithm recorded a decease in path planning time while the RRT algorithm recorded an increase in path planning time with an increase in UAV positional uncertainty. But, overall the path planning time for A* with respect to RRT remain 2.4 to 1.1 times longer for scenarios 1 to 3, respectively and 30% shorter for scenario 4. This results even if A* experienced a decrease and RRT experienced an increase in path planning time with the inclusion of UAV positional uncertainty.

For scenarios 1 to 3, the success rate exceeds 90% for both path planning algorithms for the whole percentage uncertainty range with approximately 5% deterioration for the RRT algorithm only. The mean success rate for A* is more than double that of RRT for the mixed case scenario. A 5% deterioration in success rate results with the inclusion of uncertainty for scenarios 1 to 3 for both path planning algorithms. No deterioration is recorded for the Mixed case scenario, for all the range of uncertainties considered.

Both path planning algorithms record a success rate in the 100% region for scenarios 1 to 3 through the whole uncertainty range. The A* algorithm produces longer paths in longer planning time with respect to the RRT algorithm. As uncertainty increases, path planning performance deteriorates, especially for the RRT algorithm. The success rate of the RRT algorithm is only half that of the A* algorithm in the mixed case through the whole uncertainty range considered even though the A* algorithm produced longer paths.

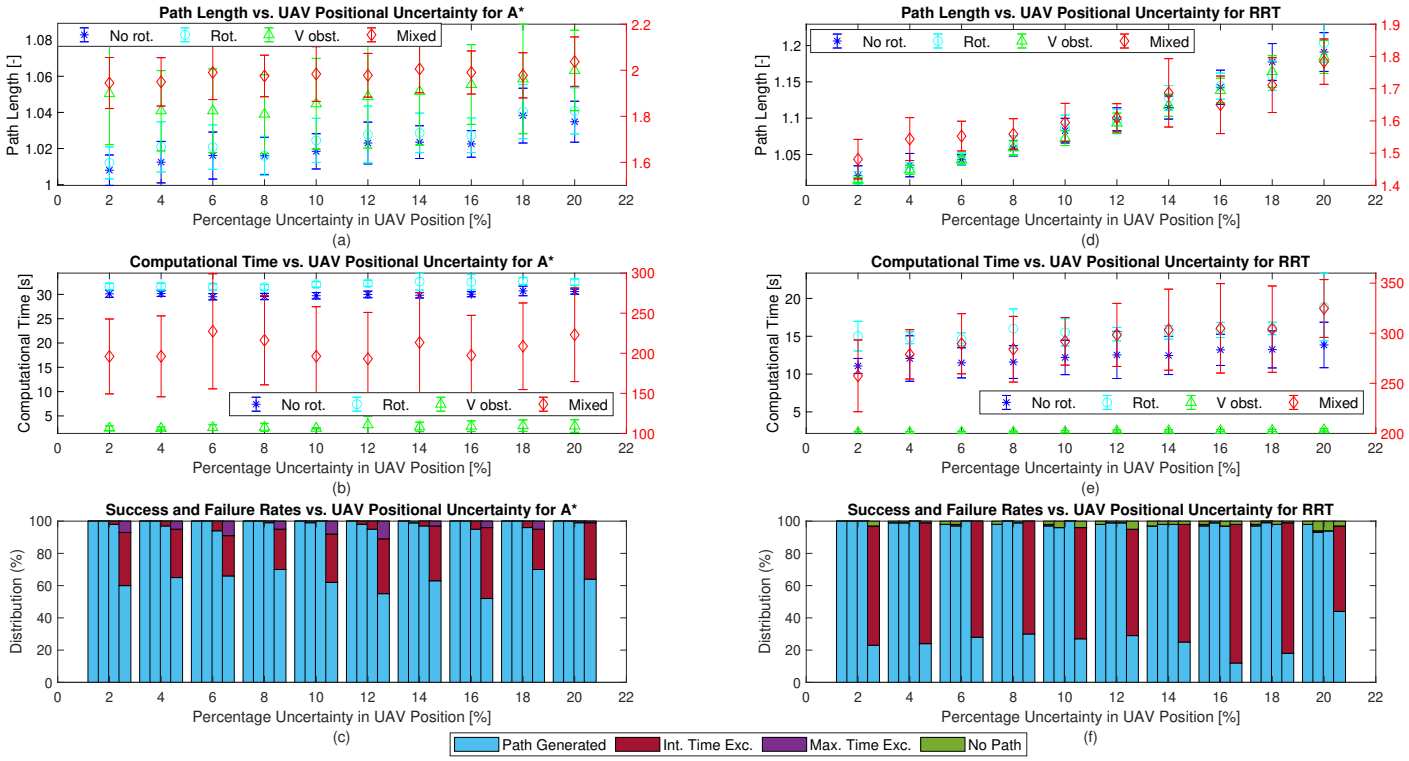

Fig. 5. Performance parameters vs. UAV positional uncertainty: (a) Path Length, (b) Computational Time, (c) Success rates for A* and (d) Path Length, (e) Computational Time and (f) Success rates for RRT for 100 iterates with 95% confidence interval. The left side black vertical axis relates to the non-rotating cube, rotating cube and rotating V-obstacle case while the right side, red vertical axis relates to the Mixed case. The set of four columns in (c) and (f) represent the non-rotating cube, rotating cube, rotating V-obstacle and the Mixed case scenarios.

5.3. *A* and RRT with uncertainty in obstacle position and orientation*

The path planning performance of both A* and RRT algorithms over a range of obstacle uncertainties is shown in Figure 6. For 3D shapes, namely cubes, the obstacle uncertainty bound is a function of the obstacle volume. For the other 2D shapes, same shape uncertainty bounds that fully enclose the obstacle are used.

The path length results for the A* and RRT algorithms are shown in Figure 6 (a) and (d). The inclusion of obstacle uncertainty has no major effect (<2%) on the mean path length for both path planning algorithms, except in the mixed case where the success rate dropped to 0%. This outcome is contrasting with the increase in path length resulting from the inclusion of UAV positional uncertainty for both algorithms in all scenarios.

Figure 6 (b) and (e) show that for both algorithms, the non rotating cube case reaches the goal point in the lowest time followed by the rotating cube, V obstacle and mixed cases, respectively. This ranking differs for that of the no uncertainty and UAV positional uncertainty cases for both algorithms. Obstacle uncertainty reduces the free space when compared with the no uncertainty tests. This reduces the number of path planning combinations for the A* algorithm, effectively reducing computational time. For the RRT algorithm, the reduction of planning space increases the number of colliding tree branches, hence increasing the computational time required prior a non colliding tree is constructed. For the V-obstacle case both algorithms experienced an increase with respect to the no uncertainty test case, with RRT showing the larger increase, since in this case the obstacle changes from a 2D shape to a 3D one. Obstacle uncertainty in the mixed case, further reduces the already limited obstacle free space, ultimately decreasing the success rate. The A* algorithm's computational time is 2.2, 0.73 and 2.1 longer in comparison with RRT's for Scenarios 1 to 3, respectively, when obstacle uncertainty is considered. A major increase in computational time for the V obstacle and mixed case scenarios, for both A* and RRT algorithms, results when comparing obstacle uncertainty tests with UAV positional uncertainty tests.

It can be deduced from Figure 6 (c) and (f) that an almost 100% success rate results for A* and RRT algorithms,

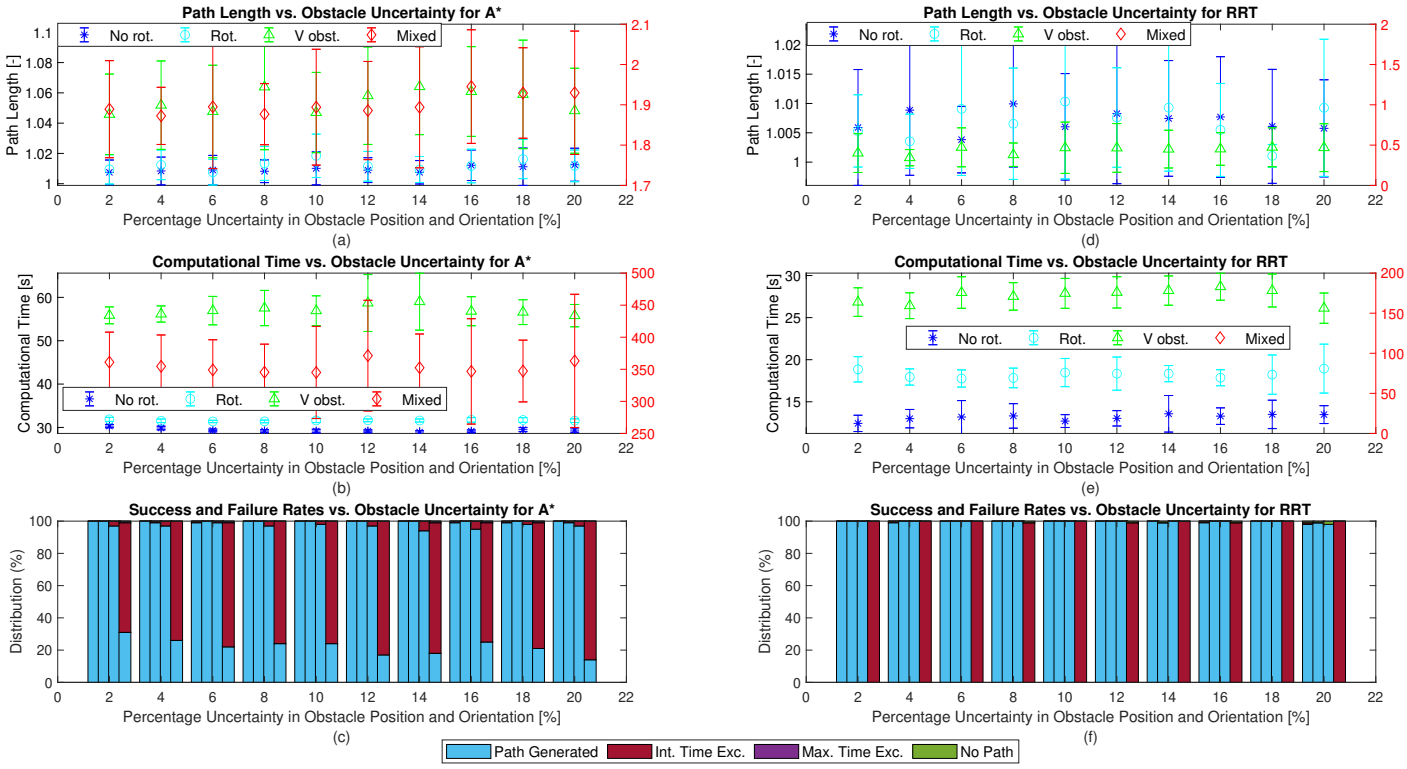

Fig. 6. Performance parameters vs. Obstacle uncertainty: (a) Path Length, (b) Computational Time, (c) Success rates for A* and (d) Path Length, (e) Computational Time and (f) Success rates for RRT for 100 iterates with 95% confidence interval. The left side black vertical axis relates to the non-rotating cube, rotating cube and rotating V-obstacle case while the right side, red vertical axis relates to the Mixed case. The set of four columns in (c) and (f) represent the non-rotating cube, rotating cube, rotating V-obstacle and the Mixed case scenarios.

for Scenarios 1 to 3. The A* and RRT algorithms exhibited a lower than 40% and a 0% success rate, respectively in the mixed case. A <5% success rate difference results when compared with the no uncertainty tests for scenarios 1 to 3 for both algorithms and a major difference (>30%) for the Mixed case scenario. Moreover, for the uncertainty range considered, results show that obstacle uncertainty exhibits a higher degradation effect on success rate than UAV positional uncertainty. The difference is only 2% for scenarios 1 to 3 in both algorithms, becoming mainly evident in the mixed case scenarios.

In conclusion, the results show that a larger deterioration results with the inclusion of obstacle uncertainty than with the inclusion of UAV positional uncertainty. The RRT algorithm exhibits the largest deterioration in path planning performance especially for V obstacles and mixed scenarios.

5.4. *A* and RRT with uncertainty in obstacle position and orientation and UAV position*

The path planning performance of both path planning algorithms in the presence of both obstacle and UAV positional uncertainties is shown in Figure 7. Both uncertainty types are modelled as explained in Section 4.4. Till now, obstacle and UAV positional uncertainties were analysed separately. Therefore, to assess their combined influence on path planning performance both uncertainties are added concurrently.

The path length for the A* and RRT algorithms are shown in Figure 7 (a) and (d), respectively. Path length results combine the responses of Figure 5 (a) and (d) (UAV positional uncertainty only)and Figure 6 (a) and (d) (obstacle uncertainty only). Path length increases with uncertainty increase for both path planning algorithms. This increase is more evident for the RRT algorithm. In comparison with the no uncertainty case, with UAV positional and with obstacle uncertainty, A* and RRT results show an minor average increase in path length (<2% for A* and

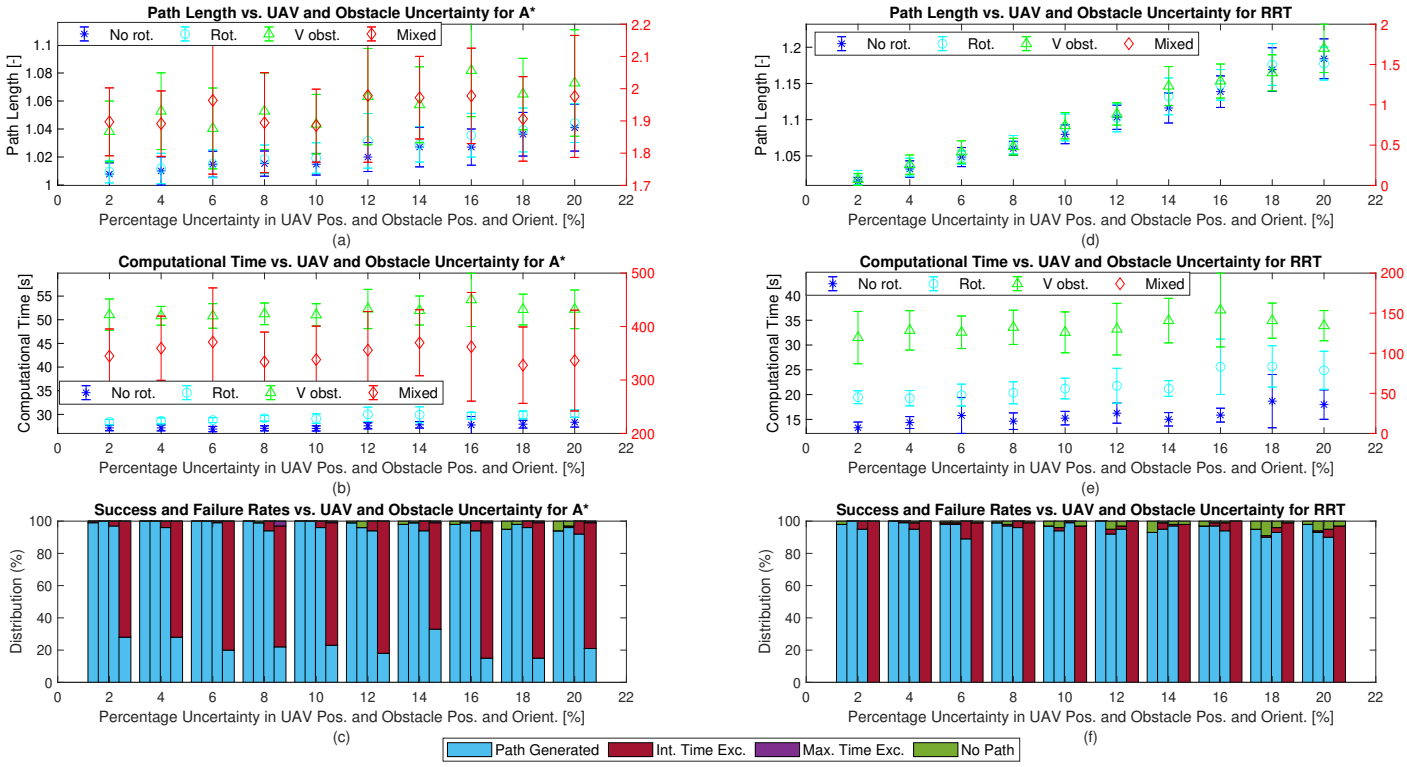

Fig. 7. Performance parameters vs. UAV positional and obstacle uncertainties: (a) Path Length, (b) Computational Time, (c) Success rates for A* and (d) Path Length, (e) Computational Time and (f) Success for RRT for 100 iterates with 95% confidence interval. The left side black vertical axis relates to the non-rotating cube, rotating cube and rotating V-obstacle case while the right side, red vertical axis relates to the Mixed case. The set of four columns in (c) and (f) represent the non-rotating cube, rotating cube, rotating V-obstacle and the Mixed case scenarios.

Table 3. Relational table between uncertainty type and path planning performance. A $\propto$ or $\propto^{-1}$ notation imply that the uncertainty type and path planning performance measure are directly or inversely proportional, respectively. An L, M and H subscript show that the effect on path planning performance due to uncertainty type being directly or inversely proportional is low, medium and high, respectively.

Parameter	Path Length		Planning Time		Success rate	
	A*	RRT	A*	RRT	A*	RRT
UAV positional uncertainty	$\propto_L$	$\propto_M$	${\propto_H}^{-1}$	$\propto_M$	$\propto_L$	$\propto_L$
Obstacle uncertainty	$\propto_L$	$\propto_L$	$\propto_L$	$\propto_H$	${\propto_H}^{-1}$	${\propto_H}^{-1}$
UAV positional and obstacle uncertainty	$\propto_L$	$\propto_M$	$\propto_L$	$\propto_H$	${\propto_H}^{-1}$	${\propto_H}^{-1}$

<10% for RRT) for all scenarios. From the results, it can be concluded that both UAV positional and obstacle uncertainties negatively influence path length, with the former having the prevalent impact.

The computational time results for the A* and RRT algorithms are shown Figure 7 (b) and (e), respectively. The computational time comparison for A* and RRT at 2% and 20% uncertainty in obstacle and UAV position show an increase for the first three scenarios and a decrease for the Mixed case scenario. This decrease is attributed to the decreasing success rate. A comparative analysis of the combined uncertainty with no uncertainty, show that both UAV positional uncertainty and obstacle uncertainties contribute to increasing computational time for both algorithms with obstacle uncertainty predominantly time consuming in V-obstacle and Mixed cases for the A* algorithm.

Figure 7 (c) and (f), show the success rate for the A* and RRT algorithms, respectively. A near 100% success rate results for both path planning algorithms for scenarios 1 to

3 throughout the range of uncertainties considered. In the mixed scenario success rate drops to 13% and 0% for A* and RRT, respectively, mirroring the obstacle uncertainty results. A comparison of these results with the no uncertainty, UAV positional uncertainty only and obstacle uncertainty only show a decrease in success rate especially for the Mixed case scenario for both path planning algorithms. Obstacle uncertainty results in the major deteriorating effect in success rate for A* while for RRT both uncertainties contribute more equally to the deterioration of the success rate.

In conclusion, the concurrent inclusion of both UAV positional and obstacle uncertainties deteriorates path planning performance, particularly for the RRT algorithm as opposed to a singular uncertainty source.

5.5. *Conclusion*

The real-time path planning performance of the A* and RRT algorithms without uncertainty, with UAV positional uncertainty, with obstacle uncertainty and with the latter two combined, in four different scenarios were presented, discussed and analysed in this section. Results show that:

(1) All uncertainties considered, deteriorate path length, computational time and success rates, especially for the RRT algorithm;
(2) The RRT algorithm constructed shorter paths in less time for the cube and V-obstacle scenarios, while the A* algorithm showed a better performance in complex scenarios;
(3) Path planning performance is deteriorated differently by different uncertainties;
(4) The concurrent inclusion of both UAV positional and obstacle uncertainties further deteriorate path planning performance, particularly for the RRT algorithm.

This study affirms that the neglect of uncertainties in 3D UAV path planning, particularly in complex environments, can undermine the safety and effectiveness of the UAV and the environment in which it operates.

Table 3 summarises the results presented in this section by showing the effect of each uncertainty type and their combined effect on path planning performance. A $\propto$ or $\propto^{-1}$ notation imply that the uncertainty type and path planning performance measure are directly or inversely proportional, respectively. Additionally, the subscripts L, M and H show that the effect on path planning performance due to uncertainty type being directly or inversely proportional is low, medium and high, respectively.

6. Conclusion and Future Work

This study discussed 3D UAV real-time path planning performance of a state-of-the-art graph-based (A*) and a sampling-based (RRT) algorithm in different complexity dynamic environments with UAV positional and obstacle uncertainties. The need for consideration of dynamic environments and uncertainty in path planning for UAV is specifically demanded in literature. Four main uncertainty sources are identified in literature. For the scope of this study, these are integrated into UAV positional and obstacle positional and orientation uncertainties. The bounded shape technique is used to model these uncertainties. The path planner parameters, the UAV model and four scenarios are developed based on real UAV implementations. Both UAV positional and obstacle uncertainties are range from 2% to 20%. Path planning performance is assessed using path length, computational time and success rates.

This study concludes that the path planning performance is hindered by both UAV positional and obstacle uncertainties in all scenarios, for both A* and RRT algorithms. Path planning performance is further hindered if both uncertainties are included at the same time. The RRT algorithm's path planning performance is the worse effected by all the uncertainties considered. The RRT algorithm constructed shorter paths in less path planning time for an equivalent (>95%) success rate with respect to the A* algorithm for all cases except the mixed scenario. In the latter scenario, A* performed better while RRT's success rate dropped to 0%. Paths constructed by the RRT algorithm pass nearer to obstacles, creating a higher collision risk than those constructed by the A* algorithm. Although each path planning method has its generic inherent characteristics, the selection of a path planning algorithm over another requires a thorough analysis of the mission requirements, environment and UAV model. Therefore, it is highly difficult to generically state in absolute terms that a path planning method is better than another. This study concludes that both A* and RRT algorithms are potential candidates for 3D real-time UAV path planning in dynamic, uncertain and low obstacle density scenarios. For more complex environments, success rate drops, particularly for RRT, since path planning time increases. Therefore, the application of both A* and RRT algorithms in complex scenarios will require a multiple times increase in computational resources as opposed to that required for low occupancy, low speed obstacle scenarios.

Future analysis shall focus on the relationship between path planning performance and the distance to travel per iterate, the look-ahead distance and the total path planning time. The integration of a 3D real-time A* and RRT based path planning algorithm into a real UAV navigation system, operating in an indoor environment shall be considered as the ultimate aim.

References

[1] M. Lan, S. Lai, T. H. Lee and B. N. Chen, A Survey of Motion and Task Planning Techniques for Unmanned Multicopter Systems, *Unmanned Systems* **9**(2) (2021) 165—198.

[2] C. Goerzen, Z. Kong and B. Mettler, A Survey of Motion Planning Algorithms from the Perspective of Autonomous UAV Guidance, *J. Intelligent & Robotic Systems* **57** (2010) 65—100.

[3] N. Dadkhah and B. Mettler, Survey of Motion Planning Literature in the Presence of Uncertainty: Considerations for UAV Guidance, *J. Intelligent & Robotic Systems* **65** (2012) 233—246.

[4] F. Vanegas and L. F. Gonzalez, Uncertainty based online planning for UAV target finding in cluttered and GPS-denied environments, in *IEEE Aerospace Conf.*, (Big Sky, MN, 2016), pp. 1–9.

[5] A. Chakrabarty and J. W. Langelaan, Energy maps for long-range path planning for small-and micro-uavs, in *AIAA Guidance, Navigation and Control Conf.*, (Chicago, IL, 2009), pp. 1–13.

[6] R. Benenson, S. Petti, T. Fraichard and M. Parent, Integrating perception and planning for autonomous navigation of urban vehicles, in *IEEE Int. Conf. on Intelligent Robots and Systems (IROS)*, (Beijing, China, 2006), pp. 98–104.

[7] P. Yao, H. Wang and Z. Su, Real-time path planning of unmanned aerial vehicle for target tracking and obstacle avoidance in complex dynamic environment, *J. Aerospace Science and Technology* **47** (2015) 269—279.

[8] C. Zammit and E. J. van Kampen, Comparison between A* and RRT Algorithms for 3D UAV Path Planning, *Unmanned Systems* **10**(1) (2022) 1—18.

[9] C. Zammit and E. J. van Kampen, Comparison between A* and RRT Algorithms for UAV Path Planning, in *Proc. AIAA Guidance, Navigation and Control Conf. AIAA SciTech Forum*, (Kissimmee, FL, 2018), pp. 1–23.

[10] C. Zammit and E. J. van Kampen, Advancements for A* and RRT in 3D path planning of UAVs, in *AIAA Guidance, Navigation and Control Conf.*, (San Diego, CA, 2019), pp. 1–17.

[11] C. Zammit and E. J. van Kampen, Comparison of A* and RRT in real-time 3D path planning of UAVs, in *AIAA Guidance, Navigation and Control Conf.*, (Orlando, FL, 2020), pp. 1–25.

[12] J. L. Foo, J. Knutzon, V. Kalivarapu, J. Oliver and E. Winer, Path Planning of Unmanned Aerial Vehicles using B-Splines and Particle Swarm Optimization, *J. Aerospace Computing, Information, and Communication* **6**(4) (2009) 271–290.

[13] K. P. Bollino and L. R. Lewis, Collision-Free Multi-UAV Optimal Path Planning and Cooperative Control for Tactical Applications, in *AIAA Guidance, Navigation and Control Conf.*, (Honolulu, HI, 2008), pp. 1–18.

[14] J. S. Dittrich, F.-M. Adolf, A. Langer and F. Thielecke, Mission Planning for Small UAV Systems in Uncertain Environments, in *2nd European Micro Aerial Vehicle Conf.*, (Braunschweig, Germany, 2006).

[15] J.-W. Lee, B. Walker and K. Cohen, Path Planning of Unmanned Aerial Vehicles in a Dynamic Environment, in *Infotech@Aerospace*, (St. Louis, Missuori, 2011), pp. 1–19.

[16] L. Swartzentruber, J. L. Foo and E. H. Winer, Three-dimensional multi-objective uav path planner using terrain information, in *50th AIAA/ASME/ASCE/AHS/ASC Structures, Structural Dynamics, and Materials Conf.*, (Palm Springs, CA, 2009), pp. 1–19.

[17] P. P. Wu, D. Campbell and T. Merz, Multi-Objective Four-Dimensional Vehicle Motion Planning in Large Dynamic Environments, *IEEE Trans. on Systems, Man and Cybernetics- Part B Cybernatics*, **41**(3) (2011) 621–634.

[18] P. Yap, N. Burch, R. Holte and J. Schaeffer, Block A*: Database-driven search with applications in any-angle path-planning, in *Proc. Conf. of Artificial Intelligence (AAAI)*, (San Francisco, CA, 2011), pp. 120–125.

[19] T. T. Mac, C. Copot, D. T. Tran and R. D. Keyser, Heuristic approaches in robot path planning: A survey, *J. Robotics and Autonomous Systems*, **86** (2016) 13–28.

[20] Y. Singh and S. Sharma, Optimal path planning of unmanned surface vehicles, *Indian J. Geo-Marine Sciences*, **47**(7) (2018) 1325–1334.

[21] J. N. Amin, J. D. Boskovic and R. K. Mehra, A Fast and Efficient Approach to Path Planning for Unmanned Vehicles, in *AIAA Guidance, Navigation and Control Conf.*, (Keystone, CO, 2006), pp. 1–9.

[22] C. Chawla and R. Pahdi, Neuro-Adaptive Augmented Dynamic Inversion Based PIGC Design for Reactive Obstacle Avoidance of UAVs, in *AIAA Guidance, Navigation, and Control Conf.*, (Portland, OR, 2011), pp. 1–25.

[23] M. Gros, A. Schöttl and W. Fichter, Spline and OBB-based Path-Planning for Small UAVs with the Finite Receding-Horizon Incremental-Sampling Tree Algorithm, in *AIAA Guidance, Navigation and Control Conf.*, (Boston, MA, 2013), pp. 1–17.

[24] Y. Kuwata, J. Teo, S. Karaman, G. Fiore, E. Frazzoli and J. P. How, Motion Planning in Complex Environments using Closed-loop Prediction, in *AIAA Guidance, Navigation and Control Conf.*, (Honolulu, HI, 2008), pp. 1–22.

[25] M. Radmanesh, M. Kumar, P. H. Guentert and M. Sarim, Overview of Path-Planning and Obstacle Avoidance Algorithms for UAVs: A Comparative Study, *Unmanned Systems*, **6**(2) (2018) 95–118.

[26] A. Short, Z. Pan, Z. Larkin and S. van Duin, Recent Progress on Sampling Based Dynamic Motion Planning Algorithms, in *IEEE Int. Conf. Advanced Intelligent Mechatronics (AIM)*, (Alberta, Canada, 2016), pp. 1305–1311.

[27] J. Larson, M. Bruch and J. Ebken, Autonomous navigation and obstacle avoidance for unmanned surface vehicles, in *Defense and Security Symposium, SPIE Conf.*, (Orlando, FL, 2006), pp. 1–12.

[28] H. Yu, R. W. Beard and J. Byrne, Vision-based Navigation Frame Mapping and Path Planning for Micro Air Vehicles, in *AIAA Guidance, Navigation, and Control Conf.*, (Chicago, IL, 2009), pp. 1–10.

[29] F.-M. Adolf, F. Andert and J. G. F. Rocha, Rapid Online Path Planning Onboard A VTOL UAV, in *AIAA Infotech, Aerospace Conf.*, (Atlanta, GA, 2010), pp. 1–11.

[30] J. Seok, M. Faied and A. Girard, Unpredictably Dynamic Environment Patrolling, *Unmanned Systems*, **5**(4) (2017) 223–236.
[31] M. Likhachev, D. Ferguson, G. Gordon, A. Stentz and S. Thrun, Anytime search in dynamic graph, *Artificial Intelligence*, **172**(14) (2008) 1613—1643.
[32] J.K. Howlett, G. Schulein and M. H. Mansour, A Practical Approach to Obstacle Field Route Planning for Unmanned Rotorcraft, in *60th Annual Forum at the American Helicopter Society*, (Baltimore, MD, 2004).
[33] A. K. Tripathi and R. Padhi, Reactive Collision Avoidance of UAVs with Simple Pin-hole Camera Based Passive Stereovision Sensing, *Unmanned Systems*, **4**(2) (2016) 129–153.
[34] A. Allam, A. Nemra and M. Padhi, Parametric and Implicit Features-Based UAV–UGVs Time-Varying Formation Tracking: Dynamic Approach, *Unmanned Systems*, (2021).
[35] C. Ericson, *Real-Time Collision Detection*, (Morgan Kaufmann Publisher, San Francisco, CA, 2005).
[36] G. S. Aoude, J. Joseph, N. Roy and J. P. How, Mobile Agent Trajectory Prediction using Bayesian Nonparametric Reachability Trees, in *Infotech@ Aerospace*, (St. Louis, MO, 2011), pp. 1587–1593.
[37] B. Lau, C. Sprunk and W. Burgard, Efficient grid-based spatial representations for robot navigation in dynamic environments, *Robotic Automation Systems*, **61** (2013) 1116–1130.
[38] B. Park, J. Choi and W. K. Chung, Mobile Agent Trajectory Prediction using Bayesian Nonparametric Reachability Trees, in *IEEE Int. Conf. Robotics and Automation (ICRA)*, (St. Paul, MN, 2012), pp. 180–186.
[39] S. Srikanthakumar, S. Liu and W. H. Chen, Optimization-Based Safety Analysis of Obstacle Avoidance Systems for Unmanned Aerial Vehicles, *J. Intelligent Robot Systems*, **65**(1-4) (2012) 219–231.
[40] F. Liao, S. Lai, Y. Hu, J. Cui, J. L. Wang, R. Teo and F. Lin, 3D Motion Planning for UAVs in GPS-Denied Unknown Forest Environment, in *IEEE Intelligent Vehicles Symposium*, (Gothenburg, Sweden, 2016), pp. 246–251.
[41] Y. Kim, D.-W. Gu and I. Postlethwaite, Real-time path planning with limited information for autonomous unmanned air vehicles, *Automatica*, **44**(3) (2008) 696–712.
[42] M. Hoy, A. S. Matveev and A. V. Savkin, Algorithms for collision-free navigation of mobile robots in complex cluttered environments: a survey, *Robotica*, **33**(4) (2014) Vol. 33, 463–497.
[43] S. M. LaValle, *Planning algorithms*, (Cambridge university press, Cambridge, UK, 2006).
[44] P. R. Florence, Integrated Perception and Control at High Speed, Master Dissertation, Massachusetts Institute of Technology (2017).
[45] A. Majumdar and R. Tedrake, Funnel libraries for real-time robust feedback motion planning, *Int. J. Robotics Research*, **36**(8) (2017) 947–982.
[46] S. K. Shah, C. D. Pahlajani, N. A. Lacock and H. G. Tanner, Stochastic receding horizon control for robots with probabilistic state constraints, in *IEEE Int. Conf. Robotics and Automation (ICRA)*, (St. Paul, MN, 2012), pp. 2893–2898.
[47] S. Daftry, S. Zeng, A. Khan, D. Dey, N. Melik-Barkhudarov, J. A. Bagnell and M. Hebert, Robust Monocular Flight in Cluttered Outdoor Environments, *ArXiv*, **1604.04779** (2016) 1–10.
[48] L. Matthies, R. Brockers, Y. Kuwata and S. Weiss, Stereo vision-based obstacle avoidance for micro air vehicles using disparity space, in *IEEE Int. Conf. Robotics and Automation (ICRA)*, (Hong Kong, China, 2014), pp. 3242–3249.
[49] S. Liu, M. Watterson, S. Tang and V. Kumar, High speed navigation for quadrotors with limited onboard sensing, in *IEEE Int. Conf. Robotics and Automation (ICRA)*, (Stockholm, Sweden, 2016), pp. 1484–3249.
[50] C. Fulgenzi, C. Tay, A. Spalanzani and C. Laugier, Probabilistic navigation in dynamic environment using rapidly-exploring random trees and Gaussian processes, in *IEEE Int. Conf. Intelligent Robots and Systems*, (Nice, France, 2008), pp. 1056—1062.
[51] G. Kewlani, G. Ishigami and K. Iagnemma, Stochastic mobility-based path planning in uncertain environments, in *IEEE Int. Conf. Intelligent Robots and Systems*, (St. Louis, MO, 2009), pp. 1183–1189.
[52] N. A. Melchior and K. Simmons, Particle RRT for path planning with uncertainty, in *IEEE Int. Conf. Robotics and Automation*, (Rome, Italy, 2007), pp. 1617–1624.
[53] B. Luders, M. Kothari and J. P. How, Chance constrained RRT for probabilistic robustness to environmental uncertainty, in *AIAA Guidance, Navigation, and Control Conf.*, (Toronto, Canada, 2010), pp. 1–21.
[54] F. Vanegas, D. Campbell, N. Roy, K. J. Gaston and L. F. Gonzalez, UAV tracking and following a ground target under motion and localisation uncertainty, in *IEEE Aerospace Conf.*, (Big Sky, MN, 2017), pp. 1–10.
[55] M. Z. Shah, R. Samar and A. I. Bhatti, Guidance of Air Vehicles: A Sliding Mode Approach, *IEEE Trans. on control system technology*, **23**(1) (2015) 231–244.
[56] Y. Xie, X. Zhang, L. Jiang, J. Meng, G. Li and S. Wang, Sliding-Mode Disturbance Observer-Based Control for Fractional-Order System with Unknown Disturbances, *Unmanned Systems*, **8**(3) (2020) 193–202.
[57] L. Yang, J. Qi, D. Song, J. Xiao, J. Han and Y. Xia, Survey of Robot 3D Path Planning Algorithms, *J. Control Science and Engineering*, **2016** (2016) 1–22.
[58] Z. Lihua, C. Xianghong and Y. Fuh-Gwo, A 3D collision avoidance strategy for UAV with physical constraints, *Measurement*, **77** (2016) 40–49.
[59] Z.-H. Wang, K.-Y. Qin, T. Zhang and B. Zhu, An Intelligent Ground-Air Cooperative Navigation Framework Based on Visual-Aided Method in Indoor Environments, *Unmanned Systems*, **9**(3) (2021) 237–246.
[60] J.-H. Cui, R.-X. Wei, Z.-C. Liu and K. Zhou, UAV Motion Strategies in Uncertain Dynamic Environments: A Path Planning Method Based on Q-Learning Strategy,

Applied Sciences, **8**(11) (2018) 2169.
[61] J. Li, M. Ran, H. Wang and L. Xie, A Behavior-Based Mobile Robot Navigation Method with Deep Reinforcement Learning, *Unmanned Systems*, **9**(3) (2021) 201–209.
[62] Z. Zeng, A. Lammas, K. Sammut F. He and Y. Tang, Shell space decomposition based path planning for AUVs operating in a variable environment, *Ocean Engineering*, **91** (2014) 181–195.
[63] D. Gonzàlez, J. Pèrez, V. Milanès and F. Nashashibi, A Review of Motion Planning Techniques for Automated Vehicles, *IEEE Trans. on Intelligent Transportation Systems*, **17**(4) (2016) 1135–1145.
[64] S. Ghandi and E. Masehian, Review and taxonomies of assembly and disassembly path planning problems and approaches, *CAD Computer Aided Design*, **67–68** (2015) 58–86.
[65] F. H. Tseng, T. T. Liang, C. H. Lee, L. D. Chou and H. Chao, A Star Search Algorithm for Civil UAV Path Planning with 3G Communication, in *10th Int. Conf. Intelligent Information Hiding and Multimedia Signal Processing (IIH-MSP)*, (Kitakyushu, Japan, 2014), pp. 942–945.
[66] P. E. Hart, N. J. Nilsson and B. Raphael, A Formal Basis for the Heuristic Determination of Minimum Cost Paths, *IEEE Trans. on Systems Science and Cybernetics*, **4**(3) (1968) 100–107.
[67] S. M. LaValle, Probabilistic roadmaps for path planning in high-dimensional configuration spaces, *EEE Trans. on Robotics and Automatio*, **12**(14) (1996) 566–580.
[68] S. M. Lavalle and J. J. Kuffner, Randomized kinodynamic planning, *Int. J. Robotics Research*, **20**(3) (2001) 378–400.
[69] S. M. LaValle and J. J. Kuffner, Randomized kinodynamic planning, in *Pro. IEEE Int. Conf. on Robotics and Automation*, (Detroit, MI, 1999), pp. 473–479.
[70] D. Devaurs, T. Siméon, and J. Cortés, Optimal Path Planning in Complex Cost Spaces With Sampling-Based Algorithms, *IEEE Trans. on Automation Science and Engineering*, Institute of Electrical and Electronics Engineers, **13**(2) (2015) 415–424.
[71] R. Geraerts and M. Overmars, Creating high-quality paths for motion planning, *Int. J. Robotics Research*, **26**(8) (2007) 845–863.
[72] L. Yang, J. Qi, Z. Jiang, D. Song, J. Han and J. Xiao, Guiding Attraction based Random Tree Path Planning under Uncertainty: Dedicate for UAV, in *Int. Conf. on Mechatronics and Automation*, (Tianjin, China, 2014), pp. 1182–1187.
[73] D. Rathbun, S. Kragelund, A. Pongpunwattana and B. Capozzi, An evolution based path planning algorithm for autonomous motion of a UAV through uncertain environments, in *Digital Avionics Systems Conf.*, (Irvine, CA, 2002), pp. 8.D.2-1–8.D.2-12.
[74] C. Zammit and E. J. van Kampen, 3D real-time path planning of UAVs in dynamic environments, in *AIAA Guidance, Navigation and Control Conf.*, (Nashville, TN, 2021), pp. 1–22.
[75] D. Hsu, R. Kindel, J. C. Latombe and S. Rock, Randomized kinodynamic motion planning with moving obstacles, *Int. J. Robotics Research*, **21**(3) (2002) 233–255.
[76] S. M. LaValle and R. Sharma, A Framework for Motion Planning in Stochastic Environments: Modelling and Analysis, in *IEEE lnt. Conf. on Robotics and Automation*, (Nagoya, Japan, 1995), pp. 3057–3062.
[77] P. B. Sujit and D. Ghose, Search by UAVs with Flight Time Constraints using Game Theoretical Models, in *AIAA Guidance, Navigation and Control Conf.*, (San Francisco, CA, 2005), pp. 1–11.
[78] B. Bethke, L. Bertuccelli and J. P. How, Experimental Demonstration of MDP-Based Planning with Model Uncertainty, in *AIAA Guidance, Navigation and Control Conf.*, (Honolulu, HI, 2008), pp. 1–22.
[79] K. Bollino, L. R. Lewis, P. Sekhavat and I. M. Ross, Pseudospectral Optimal Control: A Clear Road for Autonomous Intelligent Path Planning, in *AIAA Infotech Aerospace Conf.*, (Rohnert Park, CA, 2007), pp. 1–14.

Christian Zammit received his B. Eng. and M. Sc. degrees from the University of Malta, in 2011 and 2014, respectively. In 2021, he received his PhD from Delft University of Technology on UAV path planning under uncertainty. From 2011 to 2014, he was Researcher at the University of Malta, and worked on on various EU FP7 Projects. Now, he holds the position of a Senior Lecturer at Malta College of Arts Science and Technology (MCAST) and is a visiting researcher at the Control and Simulation group in Delft.

Christian Zammit is the author of 10 technical publications. His research interests include: path planning, autonomous systems, unmanned aircraft systems, uncertainty modelling and guidance systems.

Erik-Jan van Kampen received his BSc and MSc degrees in Aerospace Engineering from Delft University of Technology in The Netherlands in 2004 and 2006 respectively. In 2010 he received his PhD from Delft University of Technology on the topic of interval optimization. Since then he has been an assistant professor at the group of Control and Simulation in Delft. Erik-Jan van Kampen is the author of over 140 technical publications. His research interests include Fault Tolerant Flight Control and Reinforcement Learning.